Triplon Modes of Puddles

X. Noblin,[†] A. Buguin, and F. Brochard-Wyart*

Physico-Chimie Curie, UMR 168 Institut Curie / CNRS, 11 rue Pierre et Marie Curie 75231 Cedex 05 Paris, France
(Received 30 December 2004; published 26 April 2005)

Free fluctuations of the contact line of large drops ("puddles") of wavelength $\lambda > \kappa^{-1}$, the capillary length, cannot be seen on a solid substrate because even a small but finite hysteresis is enough to block these slow modes. We show here that vertical vibrations of the substrate (at frequency ω_E, acceleration Λ) above a threshold amplitude Λ_c release the line and excite contour oscillations (triplons). We observe harmonic modes and parametric excitations at $\omega_E/2$. We construct the phase diagram (Λ, ω_E) of these subharmonic modes and we study their growth dynamics: they slow down near the threshold of the contour instability.

Introduction.—The statics and dynamics of contact lines between a solid, a liquid, and air, in partial-wetting conditions (finite contact angle θ_E), have been extensively studied both theoretically [1–3] and experimentally [4–6]. The line elasticity energy E_q associated with an undulation of amplitude u_q and wave vector q was first constructed in [3]. The basic parameter is the capillary length $\kappa^{-1} = \sqrt{\gamma/\rho g}$ (where γ is the liquid surface tension, ρ the density, and g the gravitational acceleration). There are two regimes: (i) *Capillary regime* ($q > \kappa$), where $E_q = \frac{1}{2}\gamma\theta_E^2|q|u_q^2$. This elasticity, which cannot be described in terms of line tension, has been named "fringe elasticity" [1]. (ii) *Gravity regime* ($q < \kappa$), the drop is flat, having a thickness $e_c = 2\kappa^{-1}\sin\frac{\theta_E}{2}$ [2]. The elastic energy is more standard and described by a line tension $\mathcal{T}$: $E_q = \frac{1}{2}\mathcal{T}q^2u_q^2$ where $\mathcal{T} = \frac{4}{3}\gamma\kappa^{-1}[1 - \cos^3\frac{\theta_E}{2}]$. ($\mathcal{T} \approx \frac{1}{2}\gamma\kappa^{-1}\theta_E^2$ for $\theta_E \ll 1$). This line elasticity can be used to describe the shape of the line pinned on a single defect: at short distances, the profile decreases logarithmically; at long distance, the line should behave like a regular string decreasing linearly. However, this elastic energy is very weak and defects block the line. It explains why this triangular deformation has been seen only for a line floating on a liquid substrate [6].

The dynamics of contact lines fluctuations has been studied for both viscous [4] and inertial regimes [5,6]. (i) In the *viscous regime*, dissipation occurs mostly in the liquid wedge and is independent of q. The dispersion relation is deduced from a transfer of elastic energy into viscous dissipation. Experimentally, a liquid front is pushed until it comes into contact with a row of droplets deposited on a silanated silicon wafer [4]. The relaxation of the line, observed only for large q, is in good agreement with theoretical predictions. In that experiment, the main difficulty is to obtain model substrates, free of hysteresis. A very small contact angle hysteresis ($H = \cos\theta_r - \cos\theta_a \approx 0.1$, where θ_r = receding, θ_a = advancing contact angles) was enough to pin the line motion at low q. (ii) In the *inertial regime*, the mechanical energy is conserved: $\frac{1}{2}\mathcal{T}q^2u_q^2 = \frac{1}{2}M\omega^2u_q^2$, where M is the mass of liquid put into motion by the line fluctuation. The inertial dynamic is

more subtle because M depends upon q. The penetration of the flow is q^{-1} in both regimes, leading to $M_q \approx q^{-2}\theta_E$ in the capillary regime, and $M_q \approx q^{-1}e_c\theta_E$ in the gravity regime. The energy balance then leads to $\omega^2 \approx \theta_E\frac{\gamma}{\rho}q^3$ for both capillary and gravity regimes. These inertial line fluctuations named "triplons" have been studied with superfluid ^{4}He. Recently, the conditions of pseudo partial wetting of ^{4}He on silicon wafers, where a microscopic film smears the surface defects, have allowed Poujade *et al.* [5] to observe triplons and confirm the dispersion relation $\omega^2 \propto q^{3/2}$. Triplons have also been observed by us with large water puddles deposited on immiscible liquids of low viscosity [6]. But for floating lines, the dynamics are more complex because backflows are induced in the substrate. Our aim here is to study the triplons on *real substrates* characterized by a small but finite hysteresis. To avoid pinning the line by surface defects, we vibrate the substrate vertically. We focus mainly on triplons in the gravity regime, which appear when large drops are vibrated. For a flat drop of radius R_e and thickness e_c, the modes are discrete ($qR_e \sim m$) and the dispersion relation is (see Appendix):

$$\omega_m^2 = \mathcal{T}m(m^2 - 1)/\rho e_c R_e^3. \tag{1}$$

Note that $m = 1$ corresponds to a simple translation. For small angles ($e_c \approx \kappa^{-1}\theta_E$, $\mathcal{T} \approx \frac{\theta_E^2}{2}\gamma\kappa^{-1}$) and $m \gg 1$, we recover the scaling relation $\omega^2 \approx \theta_E\frac{\gamma}{\rho}q^3$. Such modes have been observed qualitatively for drops in rapid evaporation lying on a film of their vapor [7,8], for ultrahydrophobic substrates under vibrations [9,10] (where drops are deposited on an air cushion), and at high frequencies [11]. Most studies on vibrated sessile drops are concerned with the fixed contact line condition (see [12] and references therein) or only axisymmetric modes [13].

Methods.—We look at the oscillations of a water puddle of volume V (0.5 mL $< V <$ 3 mL) lying on a solid substrate and subjected to a vertical periodic acceleration: $a = -\omega_E^2\alpha_0\cos(\omega_E t) = -\Lambda\cos(\omega_E t)$, where α_0 and $f_E = \omega_E/2\pi$ are the amplitude and frequency of the vertical

displacement of the substrate, respectively. Ultra pure water drops are deposited on two different substrates. (i) Untreated polystyrene (PS) petri dish with $\theta_a = 92 \pm 1°$, $\theta_r = 78 \pm 1°$ and $H = 0.24$. (ii) Silicon wafer coated with an amorphous film of Teflon AF1601 with $\theta_a = 125 \pm 1°$, $\theta_r = 115 \pm 1°$ and $H = 0.15$. Our substrates are mechanically deformed to adopt a concave shape, avoiding the escape of the drop. The sample is placed in a closed vessel to reduce water evaporation and contamination. To vibrate the substrate, we use a loudspeaker linked to a power amplifier connected to a function generator (maximum vibration amplitude: 7 mm).

The vertical displacement of the substrate is measured by the deflection of a laser beam using a Position Sensitive Detector (PSD) connected to a data acquisition board. Frequency and acceleration range between 5 and 100 Hz and 0 and 1 g. The drop contour fluctuations are monitored from above with a high-speed camera (1000 frames/second), and a beam splitter provides a direct vertical illumination. The substrate and the flat parts of the drop reflect the light and appear bright, the parts of the drop with a significant interface slope appear dark (meniscus zone). The captured images are stored and analyzed to find the instantaneous position $R(\varphi)$ of the contact line in polar coordinates. We performed a Fourier transform of this function to obtain the spatial amplitude of each mode $\alpha_m = \sum_{n=0}^{N-1} R(\frac{2\pi n}{N}) e^{(2\pi i m n/N)}$ (Fig. 1). We analyzed all the images to obtain the time series $\alpha_m(t)$. For instantaneous contact angles larger than 90°, the contour observed does not correspond to the real contact line but to the maximum radius of the drop. Nevertheless, for $\theta = 120°$, the difference is small compared to the large amplitude of motion observed (2%) and is neglected.

Results.—At rest, the drop has a circular shape. At time $t = 0$ we start the excitation at a given frequency, and progressively increase the acceleration amplitude Λ. (i) First the contact line remains pinned, (ii) above a first, unbinding threshold Λ_u, the force increment on the line overcomes hysteresis ($\Lambda_u/g \simeq H/(1 - \cos\theta_E)$) and the line becomes free to move [12]. We observe a pulsation of the drop radius (mode $m = 0$): $R(t) = R_e + \Delta R(t)$ at the excitation frequency [Fig. 2(a)]. In a quasistatic approximation, at low ω_E, the thickness of the puddles is $e_c =$

$2\sqrt{\gamma/[\rho(g + \Lambda)]} \sin(\theta_E/2)$, which leads to $\Delta R/R \simeq \Lambda/(4g)$, using the conservation of the volume of the puddle ($V = \pi R^2 e_c$). A puddle, disturbed from its equilibrium radius, fluctuates at frequencies $\omega_0 \simeq \sqrt{ge_c}/R$ (mode $m = 0$), where $\sqrt{ge_c}$ is the velocity of the gravity waves on shallow water. Typically, $\omega_0 = 8$ Hz for $R = 1$ cm. As soon as $\omega_E \gtrsim \omega_0$, the quasistatic approximation does not hold anymore: ΔR becomes very large near ω_0 and falls almost to zero at higher frequencies. (iii) Above a second threshold (Λ_c), the contour becomes unstable and starts to fluctuate. During a transient period, the instability grows and reaches a stationary state corresponding to a given eigenmode m [Fig. 2(b) and 2(c)]. The mode is subharmonic, with a frequency $\omega_m = \omega_E/2$ (Fig. 3). We also observe weak harmonic resonances. For example, the harmonic mode $m = 3$ arises in the same frequency region as subharmonic mode $m = 2$: $\omega_3 \sim 2\omega_2$. In some regions of the (ω_E, Λ) diagram, we do not observe a stationary state: the regime is quasiperiodic with a low frequency modulation of the subharmonic mode amplitude. We focus now on the more remarkable features of the stationary subharmonic modes.

Transient regime: birth and growth of triplons.—In Fig. 3(a), we plot the oscillations of the puddle radius, at time $t = 0$ the vibrations begin ($\Lambda > \Lambda_c$). The contour fluctuates around R_e at ω_E, and suddenly, a subharmonic $m = 3$ mode ($\omega_3 = \omega_E/2$) starts to grow exponentially with time τ [Fig. 3(b)] up to a stationary state. Plotting $1/\tau$ versus $\Delta R/R$ [Fig. 5(b)], we find a dynamic slow down when approaching the instability threshold. We also see that the radius oscillation ΔR decreases when the mode 3 grows [Fig. 3(a)].

Stationary regime.—At fixed frequency, we increase the acceleration and we plot the amplitude of the harmonic ($m = 0$) and subharmonic modes when the stationary regime is reached. A typical plot is shown in Fig. 4(a) for
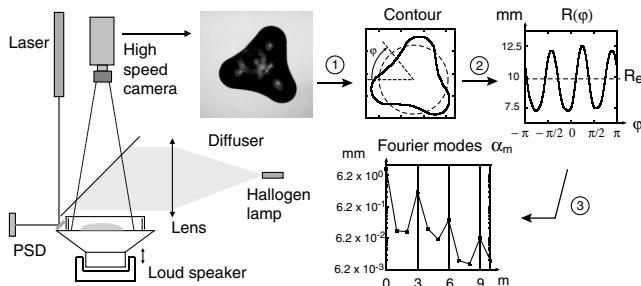
FIG. 1. Experimental setup and image analysis.
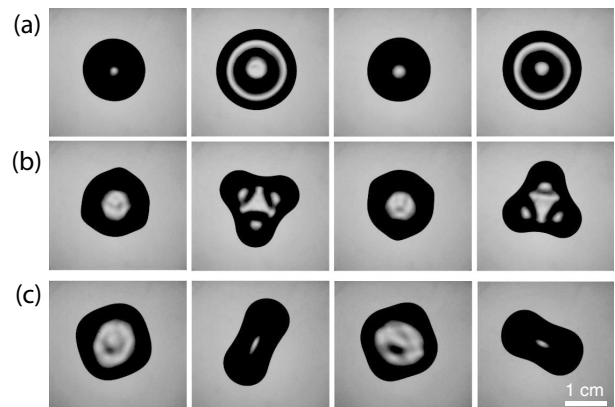
FIG. 2. (a) $f_E = 9$ Hz, harmonic variations of the drop radius: mode $m = 0$ ($\Lambda_u < \Lambda < \Lambda_c$). (b) $f_E = 9$ Hz, subharmonic mode $m = 3$ ($\Lambda > \Lambda_c$). (c) $f_E = 6$ Hz, subharmonic mode $m = 2$ ($\Lambda > \Lambda_c$). Drop radius: 1 cm. Half an excitation period between each image.
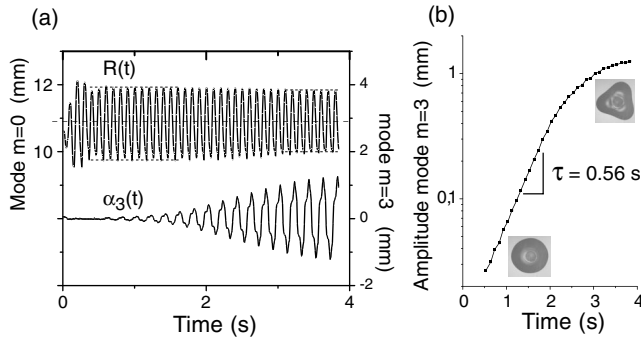
FIG. 3. (a) mode $m = 0$ (top) and $m = 3$ (bottom) amplitudes versus time ($R_e = 11$ mm, $f_E = 10$ Hz, water on PS). (b) log-linear plot of the mode 3 amplitude versus time.

FIG. 4. (a) Stationary amplitude of modes $m = 0$ (circles) and $m = 2$ (squares) ($f_E = 7.3$ Hz) in reduced units $\tilde{u} = u/R_e$ and Λ/g. (b) Stability diagram in two representations. Black squares: $3\Delta R/R$ versus f_E, hollow squares: $3\Lambda_c/4g$ versus f_E. Water on PS, $R_E = 11$ mm.

$m = 0$ and $m = 2$. Above a first threshold Λ_u (here 0.2 g), the mode $m = 0$ starts to increase; at a second threshold Λ_c (here 0.32 g), the amplitude α_2 increases rapidly. The diagram is typical of a bifurcation diagram. Above the threshold Λ_c, the mode $m = 0$ grows much more slowly. This is the signature of the coupling between mode $m = 2$ and $m = 0$ noticed previously.

Stability diagram.—We vary the frequency f_E. For each f_E we increase Λ, and we measure $\Lambda_c(f_E)$ and the amplitude ΔR at the threshold. The corresponding stability diagram for the mode $m = 2$ is shown in Fig. 4(b).

Using acceleration as a parameter, the limit of the instability region decreases with frequency. In contrast, the curve with the radius oscillation amplitude presents a minimum and looks more like a classical tongue of the parametric oscillator: under the curve, the drop remains circular and in the region above the curve (shaded areas), the drop presents shape oscillations (here mode $m = 2$). At low frequencies ($\omega_E \ll \omega_0$), the two curves are close because the quasistatic approximation holds, $\frac{\Delta R}{R_E} \approx \frac{\Lambda}{4g}$. At higher frequencies, the radius oscillations present resonance and low acceleration are sufficient to obtain a large response. We see clearly a large deviation from the quasistatic law.

Interpretation.—When we increase the amplitude of vibration of the substrate, we observe two thresholds: (i) A transition between pinned and mobile contact line occurs at $\Lambda_u/g \simeq H/(1 - \cos\theta_E)$. The harmonic pulsation of the drop above Λ_u is dominated by the axisymmetric mode $m = 0$. The amplitude becomes large when $\omega_E \sim \omega_0 \simeq \sqrt{ge_c}/R_E$ [12]. (ii) A transition between axisymmetric to non axisymmetric modes occurs above a second threshold Λ_c. The circular contour of the puddle becomes unstable: a triplon, characterized by its azimutal number m, starts and fluctuates at half the excitation frequency. This is characteristic of a parametric oscillator. The deformation of the contour around its circular shape [$R(\varphi, t) = R_e + u(\varphi, t)$] for the mode m obeys an oscillator equation (neglecting all dissipation effects): $\ddot{u} + \omega_m^2 u = 0$ where

$\omega_m^2 = \frac{m(m^2-1)\mathcal{T}}{\rho e_c R_e^3}$. The coupling between triplons and vertical vibrations comes from the fluctuations of $R(t)$. Expanding $\omega_m(R_e + \Delta R \cos\omega_E t)$, we obtain

$$\ddot{u} + \omega_{m0}^2(1 + h\cos\omega_E t)u = 0 \qquad (2)$$

where ω_{m0} is the eigenfrequency for $R = R_e$ and $h = 3\Delta R/R$. This is the classical equation of a parametric oscillator [14] where the eigenmode frequency is a periodic function of time. If $\omega_E \ll \omega_0$, the fluctuations of $R(t)$ are quasistatic and $h \simeq 3\Lambda/4g$ is proportional to the amplitude of acceleration. If $\omega_E \gtrsim \omega_0$, the parametric coupling $3\Delta R/R$ is measured experimentally. In the stability diagram (Fig. 4) we used values of the radius oscillations in the permanent regime for ΔR. Some solutions of Eq. (2) are unstable modes at a frequency $\omega_E/2$ very close to ω_{m0}: $\alpha = \alpha_0 e^{st} \cos[(\omega_{m0} + \epsilon/2)t]$ with $\omega_E = 2\omega_{m0} + \epsilon$, $\epsilon \ll \omega_{m0}$ and $s = 1/2\sqrt{(h\omega_{m0}/2)^2 - \epsilon^2}$. Parametric resonance ($s > 0$) occurs in the range $-h\omega_{m0}/2 < \epsilon < h\omega_{m0}/2$ (straight lines in Fig. 5). If we compare our measurements with the theory for mode $m = 2$, we find that measured thresholds are below expected. It can be explained by the decrease of ΔR induced by the growth of the m mode shown in Fig. 3. By plotting the maximum amplitudes $3\Delta R_{max}/R$ measured before the instability, we find a good agreement with the theory (Fig. 5). For ω_E close to $2\omega_{m0}$, the threshold has a finite value related to dissipation effects.

The phenomenon of parametric resonance is maintained in the presence of slight friction, but the domain of instability is reduced. In our case, we have two dissipative processes: (i) the viscous dissipation in the boundary layer and (ii) the hysteresis, acting as solid friction. This adds two contributions to Eq. (2):

$$\ddot{u} + \omega_m^2(1 + h\cos\omega_E t)u + \lambda\dot{u} + \mu\,\text{sgn}(\dot{u}) = 0 \qquad (3)$$

where $\lambda = \eta/\rho e_c \ell_\omega$ ($\ell_\omega = \sqrt{\eta/\rho\omega_m}$ is the penetration length) and $\mu = \gamma H m/\rho e_c R_E$ is the hysteretic friction (sgn$\dot{u} = 1$ if $\dot{u} > 0$ and -1 if $\dot{u} < 0$). The third term
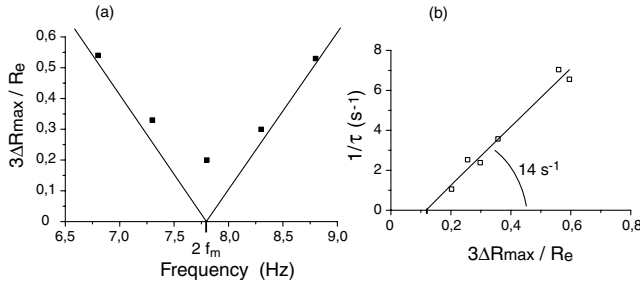
FIG. 5. (a) Stability diagram $3\Delta R_{max}/R$ versus f_E. (b) $1/\tau$ versus $3\Delta R_{max}/R$, 8 Hz, τ diverges at threshold. Water on Teflon, $R_e = 9.3$ mm.

in Eq. (3) leads to a damping of the mode $e^{st}e^{-\lambda t}$. The limit of instability becomes $s - \lambda > 0$, leading to $\epsilon^2 < h^2\omega_{m0}^2/4 - \lambda^2$. The resonance does not appear any more for arbitrarily small h values. The fourth term (hysteresis) is more subtle. Instead of causing an exponential damping, the mode amplitude α decreases linearly ($d\alpha/dt = s\alpha - V$, $V = 2\mu/\pi\omega_m$). The growth of α becomes $\alpha - V/s = (\alpha_0 - V/s)e^{st}$. The mode grows only if $s\alpha_0 > V$. At large amplitude of vibration, the stability diagram corresponding to $s = 0$ can be approximated by $-3\Delta R\omega_m/(2R_e) < \epsilon < 3\Delta R\omega_m/(2R_e)$ and $s \sim 3\Delta R\omega_m/(4R_e)$. On the other hand, when $\Lambda \to \Lambda_c$ ($s - \lambda \to 0$), the growth time diverges $1/\tau = s - \lambda$. At the frequency $\omega_E = 2\omega_{m0}$, $1/\tau = 3\Delta R\omega_{m0}/(4R_e) - \lambda$. We plot $1/\tau$ versus $h = 3\Delta R_{max}/R$ (maximum radius oscillations amplitude) for various ω_E [Fig. 5(b)]; we find a linear dependance with a slope equals to 14 s^{-1} which is close to twice the predicted value ($\omega_{m0}/4 = 6.3$ s^{-1}). In fact, as for critical phenomena described by the Landau mean field Hamiltonian [15], the critical relaxation frequencies above and below the critical temperature differ by a factor of 2.

Conclusion.—The vertical vibrations of sessile puddles lead to oscillations of the drop radius (mode 0), which induce parametric instabilities of the contour, called subharmonic triplons. We measure their characteristics (growth time, amplitude, stability diagram). Our results are the following: (i) The control parameter is the amplitude ΔR of the mode 0, not the acceleration Λ of the substrate. At low frequencies ($\omega \ll \omega_0$), the puddle has time to follow the modulation of the vertical acceleration; then the two parameters are equivalent. But at higher frequencies, the quasistatic approximation does not hold anymore: the response $\Delta R/R$ becomes much larger near resonance ($\omega \sim \omega_0$) and falls down to very small values at higher frequencies. (ii) Slow down of the growth time near threshold. We made the first experimental measurement of $1/\tau$ versus $\Delta R/R$. The divergence of τ near threshold is typical of this phenomenon. (iii) Even for small contact angles, the contour instability appears. (iv) When a mode m becomes unstable and starts to grow, the amplitude of mode 0 (source of the instability) decreases, leading to

permanent regimes studied here, but also more complex spatiotemporal behaviors (oscillatory or chaotic) which will be studied later.

Appendix.—A large flat drop (thickness e_c) can be described as a 2D film [6]. A deformation of the contour gives rise to a surface pressure Π given by a Laplace law extended to 2D ($\Pi = \frac{\mathcal{T}}{R}$), where R is the curvature radius. For a modulation of the contour ($R_c = R_e + u$), the curvature is $\frac{1}{R} = \frac{1}{R_e} - \frac{u+\ddot{u}}{R_e^2}$, where $\ddot{u} = \frac{d^2u}{d\theta^2}$. In the inertial regime, the flows are plug flows ($\vec{v}_p$). The fundamental equation is $\rho e_c \frac{\partial V}{\partial t} = -\nabla_p\Pi$ and the conservation of area leads to $\Delta\Pi = 0$. For a deformation $u = u_0 \cos m\theta e^{i\omega t}$, this leads to $\Pi = \Pi_S r^m$, with $\Pi_S = \frac{1}{R_e} + (m^2 - 1)\frac{u}{R_e^2}$ and to the dispersion relation Eq. (1).

---

[1] P. G. de Gennes, Rev. Mod. Phys. **57**, 827 (1985).
[2] P. G. de Gennes, F. Brochard-Wyart, and D. Quere, *Capillarity and Wetting Phenomena: Drops, Bubbles, Pearls, Waves* (Springer, New York, 2003).
[3] J. F. Joanny and P. G. de Gennes, J. Chem. Phys. **81**, 552 (1984).
[4] T. Ondarçuhu and M. Veyssié, Nature (London) **352**, 418(1991).
[5] M. Poujade, C. Guthmann, and E. Rolley, Europhys. Lett. **59**, 862 (2002).
[6] X. Noblin, A. Buguin, and F. Brochard-Wyart, Langmuir **18**, 9350 (2002).
[7] K. Adachi and R. Takaki, J. Phys. Soc. Jpn. **53** 4184 (1984).
[8] D. E. Strier, A. A. Duarte, H. Ferrari, and G. B. Mindlin, Physica A (Amsterdam) **283**, 261 (2000).
[9] P. Aussillous and V. Bergeron, (private communication).
[10] N. Yoshiyasu *et al.*, J. Phys. Soc. Jpn. **65** 2068 (1996).
[11] Vukasinovic *et al.*, Phys. Fluids **13**, S14 (2001).
[12] X. Noblin, A. Buguin,and F. Brochard-Wyart, Eur. Phys. J. E **14**, 395 (2004).
[13] N. E. Bixler and R. E. Benner, *4th International Conference on Numerical Methods in Laminar and Turbulent Flow* (Pineridge Press, Swansea, 1985) p. 1336.
[14] L. Landau and M. Lifshitz, *Mechanics* (Butterworth-Heinemann, Washington, DC, 1987), 2nd ed.
[15] The order parameter of the triplon instability is $M = R - R_e$. To describe the stationary regime, the Landau expansion can be written as $F = 1/2aM^2 + 1/4bM^4 + \ldots$ The relaxation of M, which is not a conserved quantity, is ruled by a dynamical equation $k\dot{M} = -\partial F/\partial M$. Below Λ_c, $a > 0$, a fluctuation of $M(t)$ relaxes $M = M_0 e^{-st}$, with $s = a/k$. Above Λ_c, $a < 0$, M reaches a finite value $M_0 = \sqrt{-a/b}$. The expansion of F around M_0 leads to $F = F_0 - |a|\delta M^2 + O(\delta M^4)$. The fluctuation relaxes with a frequency $2s$.